Synthesis of ZnO based nanopowders via a non-hydrolytic sol gel technique and their densification behaviour and varistor properties

Shereef Anas[1], Poothayil Mukundan[1], Ayyappan M. Sanoj[1], Viswanathan R. Mangalaraja[2], Solaiappan Ananthakumar[1,*]

[1]*Materials and Minerals Division, National Institute for Interdisciplinary Science and Technology (NIIST), CSIR, Trivandrum, 695 019 Kerala, India*

[2]*Department of Engineering Materials, University of Concepción, Concepción, Chile*

Received 3 November 2009; received in revised form 1 March 2010; accepted 9 March 2010

Abstract

Hexagonal nanocrystalline varistor grade ZnO particles with size 50 nm and the specific surface area of 28 m^2/g have been prepared by non-aqueous gelation technique involving diethylene glycol and triethanolamine. The as-prepared varistor nanopowders were analyzed with the support of XRD, TG/DTA, FTIR, TMA, SEM and TEM. Varistor discs were fabricated by pressing and their densification was studied at 850, 950, 1050 and 1150°C. The evolution of varistor microstructures, extent of grain growth and the influence of microstructure on the I-V properties were explored and presented.

Keywords*: nanocrystalline material, sintering, electrical properties, ZnO varistors*

I. Introduction

The demand for electrical energy increases steadily in developing nations like India which has definite plans to set up more nuclear and hydroelectric power plants and huge networking of power distribution lines along with mini-power stations in near future. This will bring the varistor industry to the limelight and also the need to develop high performance, high energy varistors. The industry has fixed the energy handling capability of 600 V/cm^3 as target for the new-generation ZnO-Bi_2O_3 varistor blocks within the restricted volume. The implementation of environmental safety in the industrial sector has also called for a suitable 'eco-design' for the new varistor products.

Currently available ZnO-Bi_2O_3 varistors have many drawbacks, namely exaggerated grain-growth, volatility of Bi_2O_3 liquid phase, formation of undesired reactive phases, poor stability and prolonged densification schedule [1–3]. During the sintering process, varistors additives and dopants produce macro-grained microstructures with grain sizes ranging between 15–20 μm [4]. Such large ZnO grains yield poor threshold voltage (V_b). Apart from these, a single varistor block has 40 mm × 40 mm dimensions and more than 400 g weight. These issues receive most of the attention in the design and development of state-of-the-art varistors. The immediate requirements for this concern were small-sized, light weight, sintered ZnO varistors containing fine-grained active ZnO with homogeneous distribution of insulating grain boundaries [5].

Recent reports indicate that the use of nano-grained ZnO varistors can solve the existing limitations in varistor field. Hence, varistors development involving nanoparticles was taken up by many material scientists and synthesis of varistors grade nanoparticles by novel chemical methods like sol-gel, hydrothermal, citrate gel decomposition, and microwave assisted flash combustion and urea decomposition techniques have been numerously attempted [4–7]. Homogeneous mixing of low level dopants and additives, low temperature densification, reduction in ZnO grain size and three to four times increase in the varistors performance were a few advantages realized when nano size raw material was used [4,7].

Literature studies show that the sintering of 'nano-varistors' was very critical since high surface area ZnO can undergo spontaneous grain growth. Therefore special techniques such as spark plasma sintering, two-stage densification, constrained and rate controlled sin-

* Corresponding author: tel: +91 471 2515 289
fax: +91 471 2491 712, e-mail: *ananthakumar70@gmail.com*

tering were used for retaining the sintered ZnO grains in nano scale [8,9]. These techniques are still at the laboratory research level. In conventional sintering of nano-varistors, the densification was mostly carried out at temperatures between 1000–1200°C. Although sintered density as high as 98 %TD was achieved, ZnO grain size >5 μm was frequently obtained. Recently densification of ZnO nano-varistors at low temperatures has been attempted. For example, Duran et al. [10] have used a metallorganic polymeric method for preparing varistor grade nanopowder and densification of nano-varistors between 850–940°C. Suresh and team [11] prepared miniaturized and self assembled varistor through nanopowder. In their work, the nano originated varistors were studied at a temperature of 1050°C.

Since sol-gel is a simple technique for nanoparticles synthesis, we used the same for preparing varistor nanoparticles [12]. However, when an aqueous sol-gel synthesis was applied for obtaining multi-component varistor grade nanopowder, the most important precursor additives, like bismuth and antimony salts, get hydrolyzed instantly which results in preferred precipitation and non-homogeneous powders. Therefore, a non-hydrolytic sol gel synthesis was performed in this work involving glycol and amine precursors [13]. The densification of varistor grade nanopowders at different temperatures and the corresponding microstructures and their effect on the breakdown voltage and non-linearity coefficient were analyzed and reported.

II. Experimental

2.1. Non-hydrolytic synthesis of nanopowders

Varistor composition consisting of 94 mol% ZnO, 3 mol% Bi_2O_3 and 1 mol% each of Cr_2O_3, CoO and Sb_2O_3 each, was prepared in this work. The preferred composition was found to be good for understanding the basic varistor properties [8]. Thermogelation was the technique used for making varistor gel. In a three necked reflux flask fitted with a condenser, 1.0 M zinc nitrate (99 %, Merck) precursor solution prepared in 100 ml iso-propanol (99.9 %, Ranbaxy) was refluxed using a laboratory heating mantle. When the reflux reaction temperature reached 80°C, cobalt nitrate (0.30 g) (99 %, CDH), chromium nitrate (0.42 g) (98 %, CDH) and antimony chloride (0.24 g) (98 %, S.D. fine) dissolved in 50 ml iso-propanol medium were introduced dropwise. Bismuth nitrate (1.52 g) (99 %, CDH) solution, prepared in diethylene glycol (DEG) medium (25 ml), was simultaneously added. While refluxing, triethanolamine (50 ml) (99 %, Ranbaxy) was slowly introduced into the precursor nitrates. The volume ratio of the DEG, triethanolamine and iso-propanol was maintained as 1 : 2 : 6. The precursor solution turned to a transparent viscous gel after refluxing for 105 minutes. The resultant precursor gel was collected and condensed further at 100°C in an electrical oven until a thick viscous rigid mass was obtained. It was then transferred to a 1000 ml beaker and heated at 270°C for 2 h at a rate of 3°C/min. Highly porous black ZnO based foam was finally obtained. The black foam was then ball milled in iso-propanol medium (300 ml) for a period of 2 h. So obtained black powder was washed with iso-propanol, dried at 70°C and then subjected to direct calcination at 500°C for 2 h at a heating rate of 3°C/min. Nanocrystalline varistor grade powder was finally obtained. It was preserved for the fabrication of varistor discs.

2.2. Fabrication of varistors

1.5 g of varistor grade ZnO based nanopowder was weighed and compacted at a pressure of 80 MPa into a disc with dimensions 12 mm diameter and 2 mm thickness using a hydraulic press (Lawrence & Mayo, India). The discs were sintered at temperatures ranging between 850°C and 1150°C in an electrically heated silicon carbide furnace. The details of the sintering schedule were given in Table.1. The heating rate was controlled by Libratherm temperature programmer. In all cases, after sintering, the furnace was cooled at normal furnace cooling rates. The as fabricated varistor discs were polished and electroded with silver and heated up to 600°C for 10 min, before carrying out the electrical measurements.

2.3. Characterization

The as prepared varistor grade ZnO based precursor gel and the gel calcined at 270°C and 500°C were characterized for the structural features, thermal stability, phase analysis, bulk surface area and morphology using FTIR, TG/DT, XRD, BET, SEM and TEM analytical tools respectively. FTIR spectra were recorded on a Nicolet Magna 560 FTIR (USA) spectrophotometer over the spectral range of 4000–400 cm^{-1} by KBr pellet method. Thermal decomposition behaviour was

Table 1. Details of heating cycle used for the sintering of doped ZnO samples

Sintering temperature	850°C/2h	950°C/2h	1050°C/2h	1150°C/2h
Ramp/ dwell	3°C/min up to 500°C 5°C/min up to 850°C dwelling for 2 h	3°C/min up to 500°C 5°C/min up to 850°C 10°C/min up to 950°C dwelling for 2 h	3°C/min up to 500°C 5°C/min up to 850°C 10°C/min up to 1050°C dwelling for 2 h	3°C/min up to 500°C 5°C/min up to 850°C 10°C/min up to 1150°C dwelling for 2 h

analyzed at a constant heat flow of 10°C/min in air atmosphere up to 1200°C using Shimadzu, TG/DTA-50H (Japan) instrument.

Crystalline nature and phase composition were studied by powder X-ray diffraction technique (Philips, X'pert Pro X-ray diffractometer) using Cu Kα radiation (λ = 0.154 nm). The crystallites size was calculated by the Scherer equation [14]. The bulk surface area was determined by the BET technique using Micromeritics Gemini 2370 instrument operating at liquid nitrogen temperature. Degassing of the samples was done at 200°C/2h. The morphological features were investigated by scanning electron microscopy (SEM, JEOL 5600 SL) and transmission electron microscopy (TEM-JEOL JEM 2000X). Selected area electron diffraction (SAED) patterns using TEM were also taken for identifying the polycrystalline nature of the sample.

The varistor discs fabricated from the nanopowders were characterized for the densification, density measurements, sintered microstructural features and current-voltage (I-V) properties. Densification curves were obtained using thermo-mechanical analyzer (TMA-60H Shimadzu, Japan). Cylindrical samples of size 6 mm height and 5 mm diameter were used for the TMA analysis. The test was performed up to 1300°C at a heating rate of 10°C/min. A dead load of 0.3 g was given for ensuring the contact between the measuring probe and the sample. The linear shrinkage ratio ($\Delta L/L_0$) of the sample with respect to temperature was measured. The green density was determined from the dimensional measurements. Densities of the sintered varistor pellets were measured by Archimedes method. The microstructures of the sintered varistor discs were observed on fractured surfaces after providing gold coating using SEM (JEOL 5600 SL). The average ZnO grain size was determined from the SEM micrographs by indigenously developed image analysis software. More than 300 grains were taken into account for determining the average grain size.

2.4. I-V measurements

Electrical performance of the sintered varistor was measured using a pulsed mode D.C. power supply having a built-in power source (600 Volts, Digitronics, India) with a current limit of 100 mA. The amount of current passing through the cross section of a sample was monitored for every 5 volts and the current density vs. electric field curves were plotted. From the I-V curves the breakdown voltage (V_b) and the nonlinearity coefficient (α) were determined. The α value was measured between 0.1 mA and 1 mA, using the standard relationship:

$$\alpha = (\log I_2 - \log I_1) / (\log V_2 - \log V_1)$$

where V_2 and V_1 are electric field at current I_2 and I_1, respectively.

III. Results and discussion

3.1. Characterization of precursor gel and varistor grade ZnO nanoparticles

FTIR analysis in Fig. 1 shows the complexation of the precursor metal nitrates with TEA and DEG. The broad stretching bands at 3356, 3436 and 3449 cm^{-1} in the as-prepared varistor grade precursor gel and the samples calcined at 270°C and at 500°C, respectively, indicate the presence of bonded and free hydroxyl groups [14]. The series of transmittance peaks at 1653 cm^{-1}, 1630 cm^{-1} and 1593 cm^{-1} are indicating the bending modes of –OH groups [15]. The precursor gel exhibits the characteristic stretching bands of nitrate group at 1394 cm^{-1} and 817 cm^{-1}. The nitrates decompose during calcinations and therefore these peaks are getting disappeared in the calcined samples [16,17]. The typi-

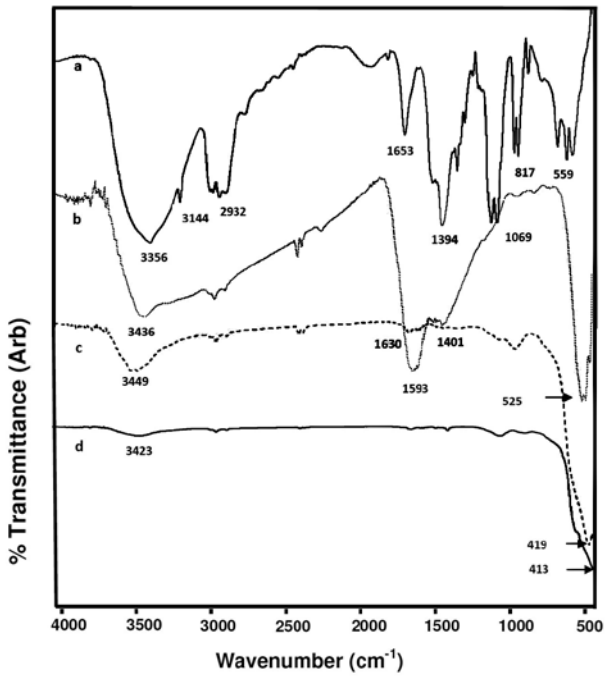

Figure 1. FTIR transmittance spectra of: varistor grade precursor gel (a), gel calcined at 270°C (b), gel calcined at 500°C (c) and ZnO powder (d)

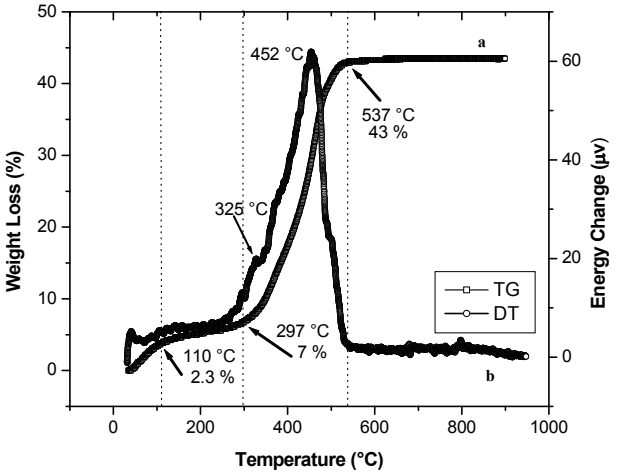

Figure 2. TG (a) DTA (b) analysis of varistor grade precursor gel

cal wavelength ranges for C-N stretches of the tertiary amines are in the range of 1250–1020 cm^{-1}. The absorption peaks in this region are also matching with the C-O-C peaks of the DEG [16,18]. It is observed that these characteristic peaks are deteriorating with increase in temperature, which confirms the removal of organic matters. Tertiary amine has weak stretching vibrations in the spectral range 3200–3000 cm^{-1} [18]. It can be seen that the shoulder peak existing at 3144 cm^{-1} in the spectrum of the precursor gel is absent in the calcined samples, due to the decomposition of the tertiary amines.

In order to confirm the formation of crystalline ZnO, the FTIR spectra of the precursor gel and the calcined powders were compared with the standard ZnO powders. In phase-pure ZnO, very intense peaks are observed in the range 600–400 cm^{-1} [15,19]. Such intense characteristic peaks are absent in the precursor gel indicating that there is no direct formation of ZnO nuclei during refluxing. It is contrary to the earlier published reports where direct formation of ZnO was reported in reflux reactions conducted in the alkaline media [8,20]. However, it is observed that the spectra taken for the gel has a red shift in the range of 600–400 cm^{-1} indicating the complex formation between zinc and the TEA-DEG complexing agents. The multiple low intense peaks in the range of 500–400 cm^{-1} for 270°C calcined gels may represent the ZnO primary seed nuclei formation. Calcination at 500°C results in the evolution of a strong peak at 419 cm^{-1} corresponding to the characteristic peak of ZnO [15,20].

TG and DTA analysis of the as-refluxed precursor gel supports the FTIR spectral interpretations. The thermogram obtained for the as-prepared varistor grade precursor gel is presented in Fig. 2. The TG curve in Fig. 2 shows three distinct decomposition steps at temperatures 110°C, 297°C and 537°C with the associated weight losses of 2.3%, 7% and 43%, respectively. The weight loss in the initial stage is significantly low, which is mainly caused by the removal of free moisture from the precursor gel. The weight loss up to 297°C is due to the degradation of CH_2OH ligands in TEA, decomposition of DEG and burning of nitrate groups from the metal nitrate precursors [21]. Moreover, release of dense yellow fumes from the gel mass is noticed nearer to 250°C confirming the decomposition of nitrates and evolution of nitrogen oxides. In fact, it is observed that the entire decomposition is accompanied by the evolution of various gaseous products such as CO, CO_2, NO and NO_2 [17]. The evaporation and decomposition of TEA are generally observed in the temperature range from 204–314°C. A large weight loss in the third stage corresponds to the decomposition of metal complexes to stable varistor grade metal oxides. Since there is no further weight loss, it is confirmed that a temperature of at least 400°C is required to convert the precursor gel into crystalline metal oxides. Differential thermal analysis again supports the thermo gravimetric results to explain the conversion of the metal complexes to metal oxides (Fig. 2). The strong exothermic peak at 452°C is associated with the decomposition of the precursor gel and formation of the stable metal oxides. Based on the TG/DTA analysis, the precursor gel was subjected to heat treatments at 400 and 500°C, respectively. The corresponding morphological changes were also noted.

At 270°C, the dehydrated precursor gel became a solid mass with a strong inter-particle network. At this temperature the gel is only partially decomposed and as a result, a hard carbonaceous foamy mass is obtained. The optical image of the foamy mass obtained is provided as inset in Fig. 3a. Since the oxide conversion is not completed at this temperature, as evidenced from FTIR and TG, the foamy polymeric mass is first ball milled and then the calcined at 400 and 500°C. The ball milling was performed for the de-agglomeration of the particles. The SEM images of the calcined ZnO varistor powders were shown in Fig 3. At 400°C, where the crystalline ZnO is only partially formed, the SEM image shows a platelet like morphology (Fig. 3a). The magnified image further reveals that there is a hexagonal array of ZnO particles within a single platelet (Fig. 3b). When

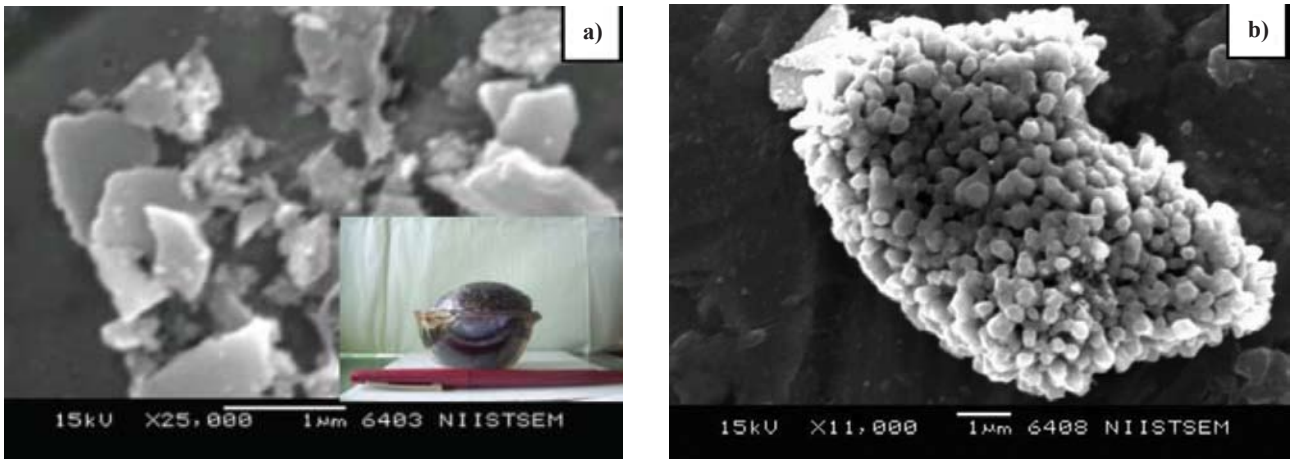

Figure. 3. Morphological features of varistor grade precursor powder at 400°C/2h: (a) platelets of nano precursors (Inset- Varistor grade foamy mass at 270°C/2h) (b) hexagonal array of ZnO in a precursor sheet

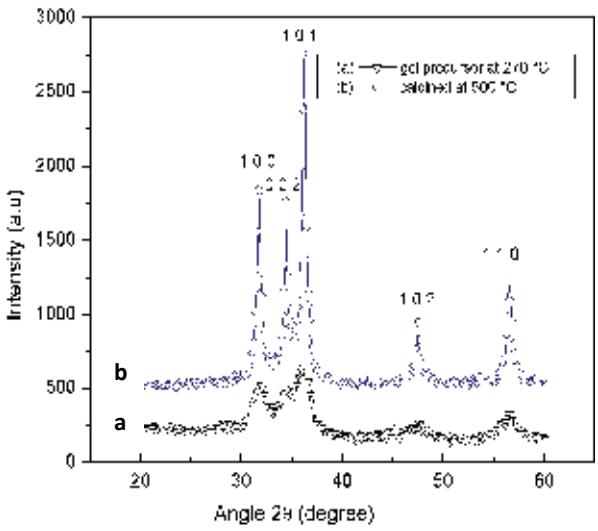

Figure 4. X-ray analysis of varistor precursors calcined (a) at 270 °C (b) and at 500°C

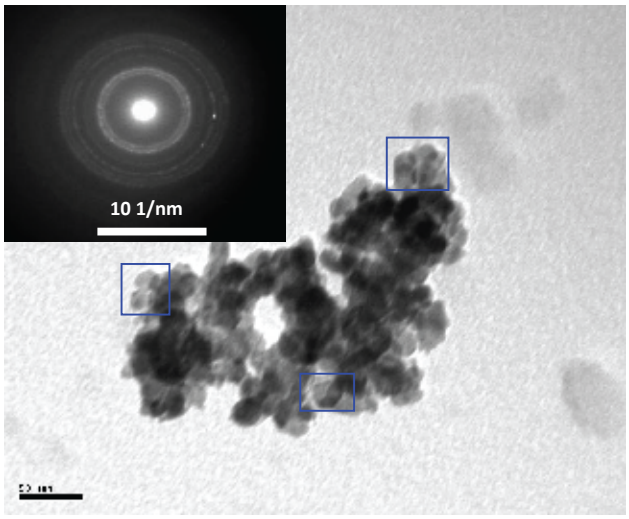

Figure 5. TEM image of the hexogonal nanoplateles of doped ZnO powder having size less than 50 nm at 500°C (Inset- SEAD of the nanopowder)

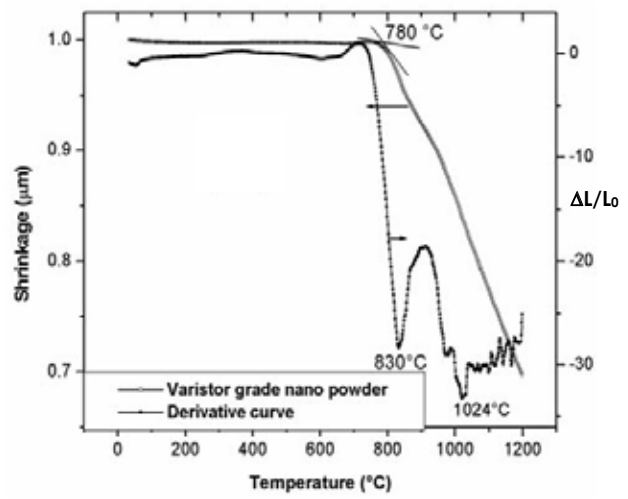

Figure 6. Sintering analysis of the varistor blocks of gel derived nanopowder

the calcination temperature is increased to 500°C/2h, fully crystalline hexagonal ZnO nanoplatelets are obtained.

The varistor precursors calcined at 270°C showed BET surface area of 32 m^2/g, whereas the direct calcination at 500°C yielded surface area of 28 m^2/g. Both these values are significantly higher compared to the conventional wet-mixed, spray granulated ZnO varistor powders (3 m^2/g) [8]. The nanopowder thus exhibit nearly ten times higher surface area than the reported conventional varistor powder, indicating that the powder is sinter-active and results in early densification upon sintering.

The powder X-ray analysis of the varistor nanopowder prepared at 270 and 500°C is presented in Fig. 4, which clearly shows semi crystalline and fully crystalline ZnO particles at 270 and 500°C, respectively. All the major peaks along the different orientations confirm the phase composition of wurtzite ZnO (hexagonal phase, space group $P6_3mc$) at both temperatures. The peaks can be assigned to (100), (002), (101), (102) and (110) planes, which is in good agreement with the standard JCPDS file for ZnO (No. 89-1397). Only for samples treated at 500°C, the XRD analysis shows the complete formation of nanocrystalline ZnO. Using Scherer equation, an average crystallite size of 11.7 nm is estimated for this powder. This value is still lower than the directly calcined aqueous sol-gel derived varistor grade nano ZnO, for which the primary crystallite size is reported as ~30 nm at 500°C [22].

The crystalline nature and morphology of the nanoparticles have been further investigated by TEM and the Fig. 5 displays the respective TEM image of the nanopowder obtained at 500°C/2h. The magnified TEM image shows the clusters of nano ZnO polyhedrons with mean size <50 nm. The selected area electron diffraction (SAED) of the nanocrystals showed ring patterns corresponding to polycrystalline wurtzite ZnO (Inset of Fig. 5).

3.2. Sintering behaviour of nanopowder compacts

The dilatometric analysis of the varistor compacts prepared from the gel derived powder is presented in Fig. 6. The dilatometric curve shows the on-set densification temperature as 780°C confirming the sintering efficiency of the nano size varistor particles. The densification was progressing up to 1024°C at a faster rate. A small step at 830°C is also observed indicating the formation of glassy liquid phase due to Bi_2O_3 [9]. We have earlier reported the sintering behaviour of spray granulated industrial grade varistor powder where the on-set densification temperature was observed only at 846°C [8]. An advantage of at least 100°C is apparently seen in the on-set densification temperature when the nanopowder is employed. The dilatometric curve further shows a gradual change in the slope indicating the

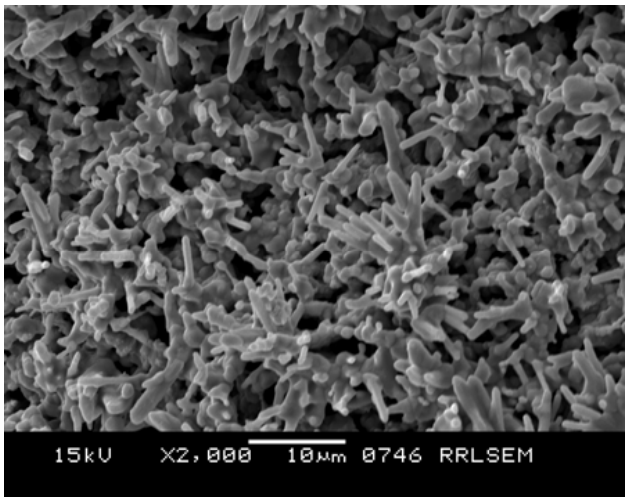

Figure 7. Microstructure of oriented growth of ZnO varistor discs sintered at 850°C

faster pore elimination and a sluggish grain growth. It may also be possible that there is a directionally oriented grain growth. This is confirmed from the SEM images of the sintered microstructures presented in Fig. 7.

Due to the nano nature and high surface area of the starting powder, a sintering temperature slightly more than the on-set densification temperature is believed to be adequate for obtaining reasonably dense varistor disc [10,23]. However, when the samples are sintered at 850°C, a porous microstructure is obtained with an oriented one dimensional ZnO growth. This further supports the results from dilatometric analysis. The ZnO grains have grown into a bunch of rods resembling the fingers (Fig. 7). Such intermediate microstructure has not been reported earlier in sol gel synthesis. The calculated sintered density at this stage is only 4.12 g/cm^3 (73 %TD). At this temperatures wetting of ZnO grains by the Bi_2O_3 liquid phase will also takes place. At 950°C, the oriented grain structure is collapsed and a characteristic hexagonal ZnO morphology is evolved (Fig. 8). In this case the average grain size was found to be < 2 µm. The sintered density also improved to 5.0 g/cm^3 (89 %TD). However, when the sintering temperature is increased to 1050°C, the increment in density is only marginal. At 1050°C the sintered density of the varistor disc was 5.1 g/cm^3 (91 %TD). However, the average grain size is found to be increased from 2 to 4 µm (Fig. 8). The grain boundaries are well formed with a clear distribution of the liquid phase along the grain boundaries. May be due to effect of grain growth, the pore elimination seems to be completed at this stage. The samples sintered at 1150°C have

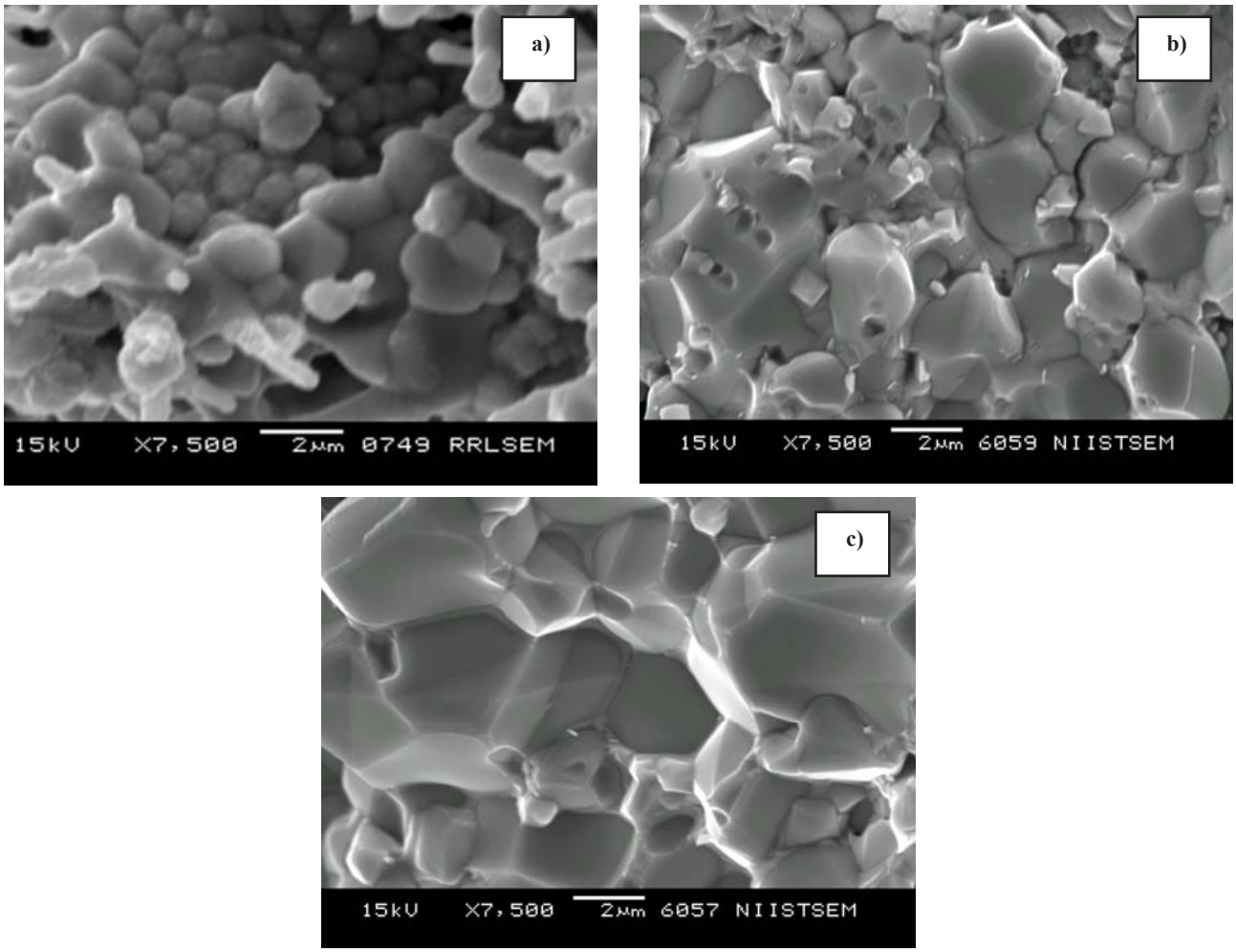

Figure 8. Microstructure of the varistors obtained by sintering at 950°C/2h (a) 1050°C/2h (b) and 1150°C/2h (c)

Table 2. Densification and electrical properties of the doped ZnO pellets with successive increments in sintering temperature

Sintering temperature	Grain Size [μm]	Density [g/cm^3]	Breakdown Voltage [V_b]	Non-Linearity Index, α
950°C/2h	< 2	5.0	557	34
1050°C/2h	< 4	5.1	493	36
1150°C/2h	< 8	5.4	323	16

sintered density of 5.4 g/cm^3 (97 %TD) with an average grain size of 8 μm (Fig. 8). Sintering of varistors beyond 1150°C was not advantageous in ZnO-Bi_2O_3 varistor system [8,24]. Therefore we restricted the sintering within 1150°C. The advantage of nanopowder is again confirmed from the sintered grain size values of ZnO. We have earlier studied the sintering behaviour of the micronized varistor powder by a solid-state process [8]. In that case, an average grain size of >15 μm was obtained at 1050°C. Whereas in the present work of gel derived nanopowder, the sintered grain size was found to be approximately three times lower under identical temperatures. Apart from the average grain size, the distribution and thickness of the glassy phase and the formation of secondary phases was also found to be critical in deciding the varistor behaviour. The X-ray diffraction analyses have been done for the varistor samples sintered at 950–1150°C. At 1150°C the presence of a week peak corresponding to $Zn_7Sb_2O_{12}$ spinel and Bi_2O_3 phases was noticed (Fig. 9).

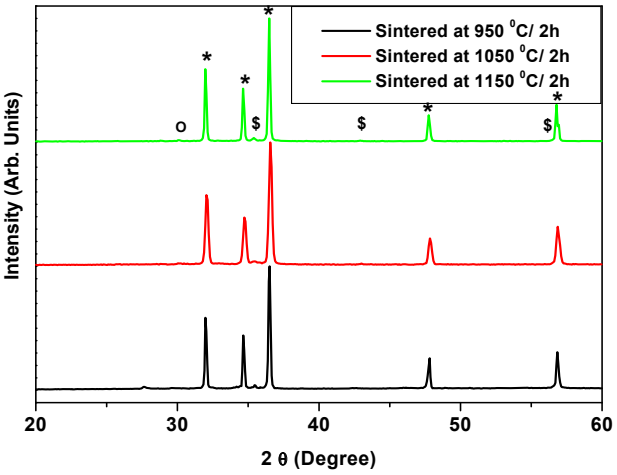

Figure 9. X-Ray diffraction patterns of ZnO nanopowder compact at various sintering temperatures (* ZnO; O Bi_2O_3; $ $Zn_7Sb_2O_{12}$)

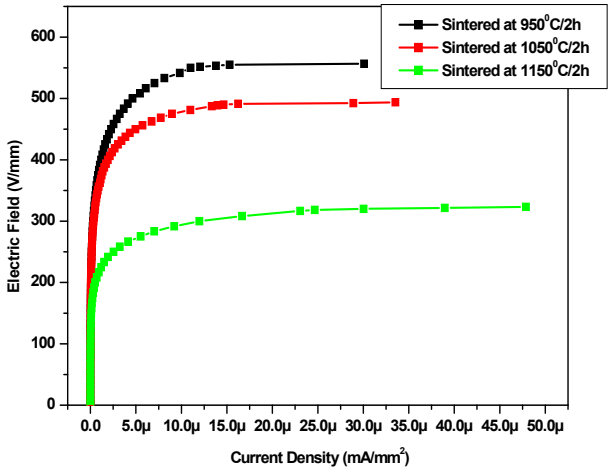

Figure 10. Current-voltage characteristics of the sintered nanopowder compact with successive increments in sintering temperature

3.3. Electrical properties of sintered compacts

In ZnO-Bi_2O_3 varistors, the electrical performance vary strongly with the number of bulk ZnO grains and the thickness of the grain boundary glassy phase. The change in breakdown voltage and nonlinearity coefficient of the varistors prepared via gel derived nanopowder with respect to the sintered density and grain size is summarized in Table 2. The linear increase in the grain size from 950 to 1150°C shows a decreasing trend in the nominal breakdown voltage. This is in accordance with the empirical relationship reported for the breakdown voltage and ZnO grain size, $V_b = m\ d/G\ V_{gb}$, where V_b is the breakdown field, d is the sample thickness, G is the average grain size and V_{gb} is the voltage across a single potential barrier and the coefficient m is averaging the potential barrier distribution [9].

The current-voltage characteristics of the sintered nano-varistors are presented in Fig. 10. The breakdown field is significantly high for the sample sintered at 950°C, where the obtained V_b value is 557 V/mm. Although the density is low at 950°C, the presence of one dimensional ZnO grains as well as the increased numbers of hexagonal shaped fine ZnO grains may be a possible reason for the high V_b value. The oriented grain structures exhibit more grain boundary area within the restricted varistor volume and may resulted in high breakdown voltage. The V_b is decreased from 493 to 323 V/mm when the sintering temperature is increased from 1050°C to 1150°C. This should be correlated to grain size increase at these temperatures. It can also be seen that the nano-varistors exhibited extended non-ohmicity irrespective to the sintering temperatures [1,25]. However, a moderate value of the leakage current (J_L) can be expected for these varistors, since the density value of all the varistors is < 97 %TD. Step-sintering and hot pressing methods were approachable methods for these varistor precursor powders, for the increased density and better varistor properties. As depicted in Ta-

ble 2, the alphas value obtained at 950°C and 1050°C were 34 and 36, respectively, for the nano origin varistors. The alpha value was found to be decreased at still higher temperatures, which may be due to the vaporization and loss of Bi_2O_3. Altogether, the study reveals that the gel derived varistor nanopowder have control in sintered ZnO grain size with respect to sintering temperature and with reasonable densification the powder offers better quality factors of the varistor like higher breakdown voltage and good non-linear properties.

IV. Conclusions

High surface area nanocrystalline varistor grade ZnO based particles with platelet morphology and an average particle size of 50 nm have been achieved through a non-hydrolytic sol-gel technique. The varistor nanoparticles have advantages as on-set densification at 746°C, one dimensional ZnO grains at 850°C, an average grain size <4 μm at 1050°C and <8 μm at 1150°C respectively with >95 %TD. The nano frame varistors with narrow grain size distribution possess higher breakdown voltage and non-linearity when compared to the reported conventional varistors, which were prepared from the spray dried varistor granules.

References

1. T.K. Gupta, "Application of zinc oxide varistors", *J. Am. Ceram. Soc.,* **73** [7] (1990) 1817–1840.
2. J. Wu, C. Xie, D. Zeng, A. Wang, "Microstructure and electrical characteristics of ZnO-B_2O_3-PbO-V_2O_5-MnO_2 ceramics prepared from ZnO nanopowders", *J. Eur. Ceram. Soc.,* **24** [14] (2004) 3635–3641.
3. I.W. Chen, X.H. Wang, "Sintering dense nanocrystalline ceramics without final-stage grain growth", *Nature,* **404** [6774] **(**2000) 168–171.
4. J. Shi, Q. Cao, Y. Wei, Y. Huang, "ZnO varistor manufactured by composite nano-additives", *Mater. Sci. Eng. B,* **99** [1] (2003) 344–347.
5. C. Leach, "Grain boundary structures in zinc oxide varistors", *Acta Mater.,* **53** [2] (2005) 237–245.
6. J. Zhang, S. Cao, R. Zhang, L. Yu, C. Jing, "Effect of fabrication conditions on I/V properties for ZnO varistor with high concentration additives by sol-gel Technique", *Curr. Appl. Phy.,* **5** [4] (2005) 381–386.
7. A.M. Hashimov, S.M. Hasanli, R.N. Mehtizadeh, K.B. Bayramov, S.M. Azizoya, "Zinc oxide and polymer-based composite varistors", *Phys. Status Solidi C,* **3** [8] (2006) 2871–2875.
8. S. Anas, R.V. Mangalaraja, P. Mukundan, S.K. Shukla, S. Ananthakumar, "Direct synthesis of varistor-grade doped nanocrystalline ZnO and its densification through a step-sintering technique", *Acta Mater.,* **55** [17] (2007) 5792–5801.
9. M. Peiteado, J.F. Fernandez, A.C. Caballero, "Varistors based in the ZnO–Bi_2O_3 system: Microstructure control and properties", *J. Eur. Ceram. Soc.,* **27** (2007) 3867–3872.
10. P. Duran, J. Tartaj, C. Moure, "Fully dense, fine-grained, doped zinc oxide varistors with improved nonlinear properties by thermal processing optimization", *J. Am. Ceram. Soc.,* **86** [8] (2003) 1326–1329.
11. S.C. Pillai, J.M. Kelly, D.E. McCormack, R. Ramesh, "Self-assembled arrays of ZnO nanoparticles and their application as varistor materials", *J. Mater. Chem.,* **14** [13] (2004) 1572–1578.
12. J. Li, S. Srinivasan, G.N. He, J.Y. Kang, S.T. Wu, F.A. Ponce, "Synthesis and luminescence properties of ZnO nanostructures produced by the sol-gel method", *J. Cryst. Grow.,* **310** [3] (2008) 599–603.
13. M.L. Kahn, M. Monge, V. Colliere, F. Senocq, A. Maisonnat, B. Chaudret, "Size and shape-control of crystalline ZnO nanoparticles: A new organometallic synthetic method", *Adv. Funct. Mater.,* **15** [3] (2005) 458–468.
14. A.R. West, *Solid State Chemistry and its Applications*, John Wiley & Sons, London, 1984.
15. B.M. Keyes, L.M. Gedvilas, X. Li, T.J. Cottus, "Infrared spectroscopy of polycrystalline ZnO and ZnO:N thin films", *J. Cryst. Grow.,* **281** [2] (2005) 297–302.
16. R.M. Silverstein, F.X. Webster, *Spectroscopic Identification of Organic Compounds*, John Wiley & Sons, Inc. New York, 1997.
17. C.C. Hwang, T.Y. Wu, "Synthesis and characterization of nanocrystalline ZnO powders by a novel combustion synthesis method", *Mater. Sci. Eng. B*, **111** [2-3] (2004) 197–206.
18. B. Smith, *Infrared Spectral Interpretation*, CRC press, Boca Raton, 1998.
19. S.R. Dhage, R. Pasricha, V. Ravi, "Synthesis of fine particles of ZnO at 100°C", *Mater. Lett.,* **59** [7] (2005) 779–781.
20. A.P.A. Oliveira, J.F. Hochepied, F. Grillon, M.H. Berger, "Controlled precipitation of zinc oxide particles at room temperature", *Chem. Mater.,* **15** [16] (2003) 3202–3207.
21. V.T. Yilmaz, Y. Topcu, A. Karadag, "Thermal decomposition of triethanolamine and monoethanolethylenediamine complexes of some transition metal saccharinates", *Thermochim. Acta*, **383** [1-2] (2002) 129–135.
22. S.C. Pillai, J.M. Kelly, D.E. McCormack, P. O'Brien, R. Ramesh, "The effect of processing conditions on varistors prepared from nanocrystalline ZnO", *J. Mater. Chem.,* **13** (2003) 2586–2590.
23. P. Duran, F. Capel, J. Tartaj, C. Moure, "Low-temperature fully dense and electrical properties of doped-ZnO varistors by a polymerized complex method", *J. Eur. Ceram. Soc.,* **22** [1] (2002) 67–77.
24. B. Balzer, M. Hagemeister, P. Kocher, L.J. Gauckler, "Mechanical strength and microstructure of zinc oxide varistor ceramics", *J. Am. Ceram. Soc.,* **87** [10] (2004) 1932–1938.
25. S.-N. Bai, T.-Y. Tseng, "Influence of sintering temperature on electrical properties of ZnO varistors"**,** *J. Appl. Phys.* **74** [1] (1993) 695–703.